



Contents lists available at ScienceDirect

Applied Surface Science

journal homepage: [www.elsevier.com/locate/apsusc](http://www.elsevier.com/locate/apsusc)



## Optical properties of LFZ grown $\beta$ -Ga<sub>2</sub>O<sub>3</sub>:Eu<sup>3+</sup> fibres

N.F. Santos<sup>a</sup>, J. Rodrigues<sup>a</sup>, A.J.S. Fernandes<sup>a</sup>, L.C. Alves<sup>b</sup>, E. Alves<sup>b</sup>, F.M. Costa<sup>a</sup>, T. Monteiro<sup>a,\*</sup>

<sup>a</sup> Departamento de Física, I3N, Universidade de Aveiro, Campus Universitário de Santiago, 3810-193 Aveiro, Portugal

<sup>b</sup> Instituto Tecnológico e Nuclear, 2686-953 Sacavém, Portugal

### ARTICLE INFO

#### Article history:

Received 29 April 2011

Received in revised form 1 July 2011

Accepted 14 July 2011

Available online xxx

#### Keywords:

LFZ

Ga<sub>2</sub>O<sub>3</sub>

Eu

PL

PLE

### ABSTRACT

Due to their relevance for electronic and optoelectronic applications, transparent conductive oxides (TCO) have been extensively studied in the last decades. Among them, monoclinic  $\beta$ -Ga<sub>2</sub>O<sub>3</sub> is well known by its large direct bandgap of  $\sim$ 4.9 eV being considered a deep UV TCO suitable for operation in short wavelength optoelectronic devices. The wide bandgap of  $\beta$ -Ga<sub>2</sub>O<sub>3</sub> is also appropriate for the incorporation of several electronic energy levels such as those associated with the intra-4f<sup>n</sup> configuration of rare earth ions. Among these, Eu<sup>3+</sup> ions (4f<sup>6</sup>) are widely used as a red emitting probes both in organic and inorganic compounds. In this work, undoped and Eu<sub>2</sub>O<sub>3</sub> doped (0.1 and 3.0 mol%) Ga<sub>2</sub>O<sub>3</sub> crystalline fibres were grown by the laser floating zone approach. All fibres were found to stabilize in the monoclinic  $\beta$ -Ga<sub>2</sub>O<sub>3</sub> structure while for the heavily doped fibres the X-ray diffraction patterns show, in addition a cubic europium gallium garnet phase, Eu<sub>3</sub>Ga<sub>5</sub>O<sub>12</sub>. The spectroscopic properties of the undoped and Eu doped fibres were analysed by Raman spectroscopy, low temperature photoluminescence (PL) and photoluminescence excitation (PLE). The Eu<sup>3+</sup> luminescence is mainly originated in the garnet, from where different europium site locations can be inferred. The spectral analysis indicates that at least one of the centres corresponds to Eu<sup>3+</sup> ions in dodecahedral site symmetry. For the lightly doped samples, the spectral shape and intensity ratio of the <sup>5</sup>D<sub>0</sub> → <sup>7</sup>F<sub>J</sub> transitions is totally different from those on Eu<sub>3</sub>Ga<sub>5</sub>O<sub>12</sub>, suggesting that the emitting ions are placed in low symmetry sites in the  $\beta$ -Ga<sub>2</sub>O<sub>3</sub> host.

© 2011 Elsevier B.V. All rights reserved.

### 1. Introduction

$\beta$ -Ga<sub>2</sub>O<sub>3</sub> is a well known wide band gap semiconductor with reported band gap energy at room temperature (RT) near 4.9 eV [1–4]. The RT thermodynamically stable monoclinic crystal has cell dimensions  $a = 1.223$  nm,  $b = 0.304$  nm,  $c = 0.580$  nm and  $\beta = 103.7^\circ$  [3,4]. The material belongs to a C<sub>2/m</sub> space group and the Ga<sup>3+</sup> ions may occupy tetrahedral or octahedral crystallographic sites [4,5]. The material exhibits isolator behaviour or n-type conductivity generally attributed to anion oxygen vacancies, the resistivity being strongly dependent on the atmosphere growth conditions [6]. However, this became controversial since recently theoretical studies [7] pointed that oxygen vacancies give rise to deep donors, with activation energies around 1.0 eV, and so cannot be responsible for the unintentional n-type conductivity observed in this oxide. Due to the above-mentioned electrical conductivity and high transparency,  $\beta$ -Ga<sub>2</sub>O<sub>3</sub> has been frequently exploited for several electronic and optoelectronic applications including electrodes as a transparent conductive oxide (TCO) [3,4]. For such purposes, information about the optically active defects and their energy

distribution inside the wide band gap host constitutes one important issue. Under above band gap excitation, ultraviolet, blue and green broad luminescence bands peaked near 3.4, 2.95 and 2.48 eV have been reported in undoped and doped  $\beta$ -Ga<sub>2</sub>O<sub>3</sub> single crystals [8–10]. The ultraviolet emission has been found to be sample independent, while deep level recombination has been found to be dependent on the chemical nature of the impurities and their content [10]. Particularly, the ultraviolet recombination has been attributed to intrinsic luminescence and the blue band has been assigned to a donor–acceptor gallium–oxygen vacancy pair recombination [9,10].

Furthermore, the wide band gap of  $\beta$ -Ga<sub>2</sub>O<sub>3</sub> makes this TCO a suitable host for phosphor applications [11–22]. As an example, high luminance was obtained in thin-film electroluminescent displays when gallium oxide is activated with europium ions [12]. However, due to poor crystallization of the gallium oxide films [13–15], the rare earth ion emission lines are very broad and little is known about the mechanisms behind the intraionic Eu<sup>3+</sup> luminescence in the crystalline Ga<sub>2</sub>O<sub>3</sub> environment. More recently, nanostructured  $\beta$ -Ga<sub>2</sub>O<sub>3</sub> has been synthesized by different routes and intentionally activated with rare earth ions for nanophosphor applications [17–22]. As for the thin films [13–15], large full width at half maximum of the main <sup>5</sup>D<sub>0,1</sub> → <sup>7</sup>F<sub>J</sub> transitions of the Eu<sup>3+</sup> ions in the nanopowders [18,20] contrast with the expected sharp lines

\* Corresponding author. Tel.: +351 234 370 824; fax: +351 234 378 197.  
E-mail address: [tita@ua.pt](mailto:tita@ua.pt) (T. Monteiro).

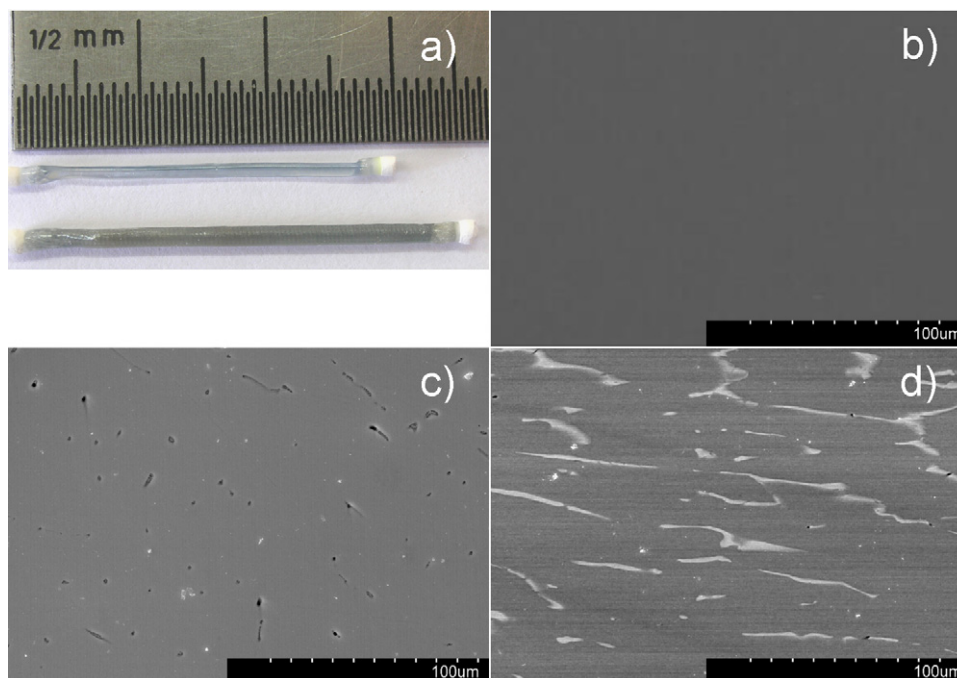


**Fig. 1.** Typical visual appearance of the (a) (top) undoped and (bottom) 0.1 mol % europium doped fibres grown at  $30 \text{ mm h}^{-1}$ . SEM micrographs of the (b) undoped fibre and europium doped fibres with (c) 0.1 mol % and (d) 3 mol % grown at  $30 \text{ mm h}^{-1}$ .

for the emitting ions in crystalline environments, from where the identification of the number of emitting Eu centres and site symmetry could be explored via the Stark level splitting due to the crystal field effect. Although the  $\text{Eu}^{3+}$  emission has been reported for thin films and nanopowders [11–22], information on the rare earth ion spectroscopic properties in bulk  $\beta\text{-Ga}_2\text{O}_3$  remains scarce and constitutes an important issue to clarify the ion properties inside this TCO material.

In the present work, undoped and Eu doped  $\beta\text{-Ga}_2\text{O}_3$  fibres were grown by laser floating zone (LFZ). The samples were characterized in what concerns their morphology and structure (SEM/EDS, PIXE, XRD, Raman spectroscopy), and their resulting low temperature optical properties (photoluminescence and photoluminescence excitation). The observed optical centres are discussed with respect to their possible phase origin and site symmetry.

## 2. Experimental details

The  $\beta\text{-Ga}_2\text{O}_3$  crystalline fibres were grown by the LFZ technique, using rod precursors for both feed and seed materials prepared by cold extrusion. These rods were obtained by using gallium (III) oxide (Alfa Aesar) powders for the undoped samples and adding 0.1% and 3.0 mol%  $\text{Eu}_2\text{O}_3$  (Aldrich) for the doped ones. The powders were mixed with polyvinyl alcohol (PVA 0.1 g/ml, Merck) in order to obtain a slurry that was further extruded into cylindrical rods with diameters of 1.75 mm.

The LFZ equipment comprises a 200 W  $\text{CO}_2$  laser (Spectron) coupled to a reflective optical set-up producing a circular crown-shaped laser beam in order to obtain a floating zone configuration with a uniform radial heating. Crystalline fibres with diameters of 1–2 mm were grown at 10 and  $30 \text{ mm h}^{-1}$  in air at atmospheric pressure. Fibre microstructure and phase development were characterized by SEM (Hitachi S4100) with energy dispersive spectroscopy (SEM/EDS) on polished surfaces of longitudinal fibre sections. Additionally, in order to obtain information on the europium distribution in the fibres, particle-induced X-ray emis-

sion (PIXE) was performed using a 2.0 MeV  $^1\text{H}$  micro beam and a  $10\text{-mm}^2$  Si (Li) detector with a resolution of 145 eV and a 5-mm Be window. The structural characterization was made by X-ray diffraction (XRD) experiments (PANalytical X'Pert PRO) and Raman spectroscopy. The latter were performed at room temperature (RT) in backscattering configuration with ultraviolet excitation by using the 325 nm line of a cw He–Cd laser (Kimmon IK Series) in a Horiba Jobin Yvon HR800 system and the 532 nm line from a Ventus-LP-50085 (Material Laser Quantum) laser in a Jobin Yvon T64000 instrument.

Steady state PL measurements were carried out at 14 K using a 1000 W Xe arc lamp coupled to a monochromator as excitation source. The luminescence was dispersed by a Spex 1704 monochromator ( $1 \text{ m}$ ,  $1200 \text{ mm}^{-1}$ ) and detected by a cooled Hamamatsu R928 photomultiplier. For the PL excitation (PLE) measurements the emission monochromator was set at the  $\text{Eu}^{3+}$  emission lines, the excitation wavelength having been scanned up to 240 nm. The spectra were corrected to the lamp and optics.

## 3. Results and discussion

The visual appearance of the undoped and Eu doped gallium oxide fibres are shown in Fig. 1a. The undoped fibre was found to be transparent while the Eu doped samples exhibit a grey colour. The morphological analysis of the fibres longitudinal sections (Fig. 1b–d) reveals, for the undoped fibre, a uniform surface without grain boundaries or second phases (Fig. 1b) regardless the pulling rate ( $10$  and  $30 \text{ mm h}^{-1}$ ). In opposition, doping induces polycrystalline nature in both lightly (0.1 mol%) and heavily (3.0 mol%) doped samples. However, the heavily doped fibres show evidence of a second phase placed at the grain boundaries (light grey contrast), while the lightly doped fibres present polycrystalline morphology with good uniformity evidencing however dispersed precipitates. The SEM images of doped fibres (Fig. 1d) show evident grain boundary features aligned with the fibre axis as a result of directional solidification characteristic of the laser

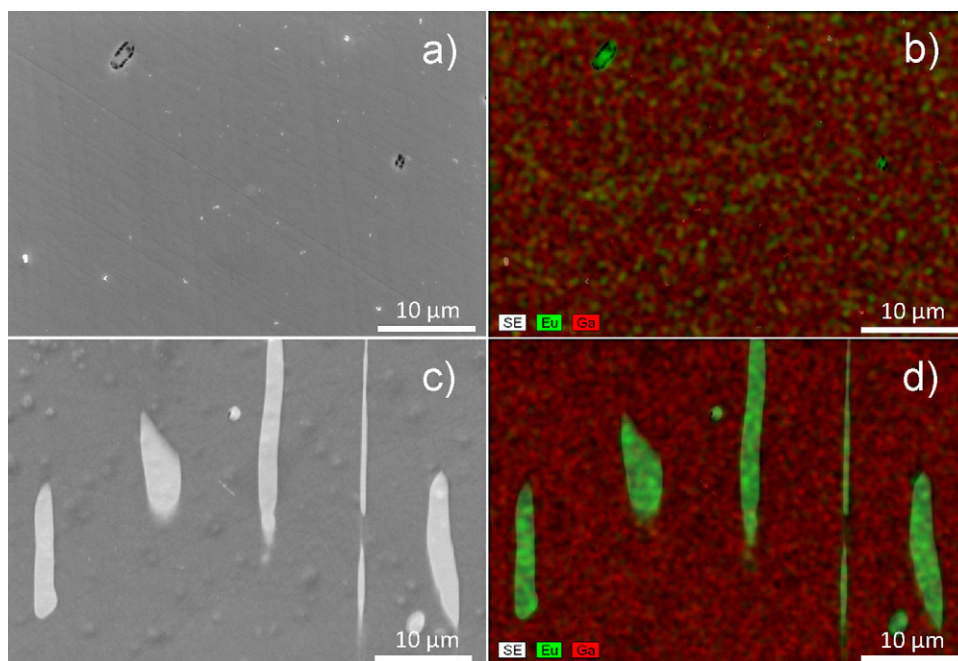


Fig. 2. SEM micrographs (a, c) and EDS maps (b, d) of the fibres grown at  $30 \text{ mm h}^{-1}$  lightly doped (a, b) and heavily doped (c, d).

floating zone growth technique. The additional contrasted regions in heavily doped fibres are due to local Eu richer crystalline phases as corroborated by PIXE (not shown), EDS (Fig. 2), XRD (Fig. 3) and Raman (Fig. 4) analysis. The peak positions of the XRD patterns of undoped and lightly doped fibres after milled into powders are in good agreement with the expected reflections from the monoclinic  $\beta\text{-Ga}_2\text{O}_3$  crystalline structure. For the heavily doped fibres, besides the  $\beta\text{-Ga}_2\text{O}_3$  crystalline structure, an additional crystalline phase was detected corresponding to the presence of europium gallium garnet,  $\text{Eu}_3\text{Ga}_5\text{O}_{12}$ . This additional crystalline phase corresponds to the clear regions in SEM with higher europium content. Since this phase could not be detected in the lightly doped samples, one can infer that the amount of Eu in these fibres is still scarce to promote the development of the garnet phase. Although europium rich precipitates were observed by SEM/EDS (Fig. 2a and b) most of the europium ions remain dispersed in the gallium oxide matrix.

The Raman active modes were observed for the LFZ fibres, either with visible (Fig. 4a and b) and ultraviolet (Fig. 4c) excitation. The measured vibrational frequencies indicated in Table 1

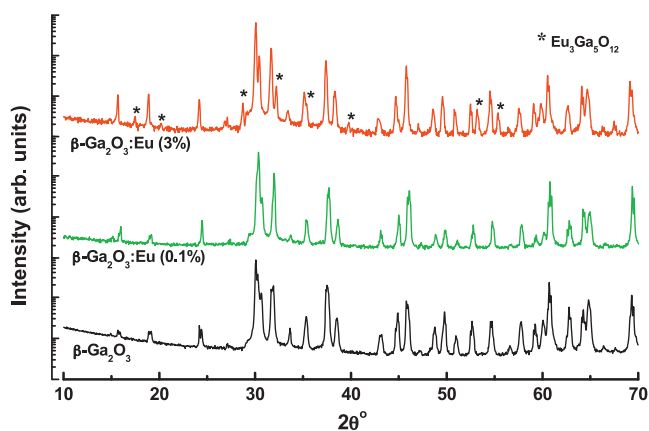


Fig. 3. XRD patterns for the undoped and doped (0.1 and 3 mol %  $\text{Eu}_2\text{O}_3$ ) fibres grown at  $30 \text{ mm h}^{-1}$ .

for both the undoped and lightly doped fibres, correspond well to the ones of the  $\beta\text{-Ga}_2\text{O}_3$  host [23,24]. The observed Raman frequencies are classified in three groups of vibrations related with librations and translations (low frequency modes up to  $\sim 200 \text{ cm}^{-1}$ ) of tetrahedra–octahedra chains, vibrations of deformed  $\text{Ga}_2\text{O}_6$  octahedra (mid frequency modes within  $310\text{--}480 \text{ cm}^{-1}$ ) and stretching/bending of the  $\text{Ga}_2\text{O}_4$  tetrahedra (high frequency modes:  $550\text{--}770 \text{ cm}^{-1}$ ) [23,24]. The Raman spectra of the undoped and lightly doped fibres are comparable as shown in spectra 1 and 2, respectively (Fig. 4a). For the heavily doped fibre (spectrum 3), additional modes at  $261 \text{ cm}^{-1}$  and  $279 \text{ cm}^{-1}$  were identified corresponding to the europium gallium garnet phase  $\text{Eu}_3\text{Ga}_5\text{O}_{12}$ , depicted in the expanded region obtained with visible excitation (Fig. 4b) [25]. The above information is summarized in Table 1. The visible Raman spectra were acquired with the samples oriented both parallelly and normally to the polarization plane of the laser

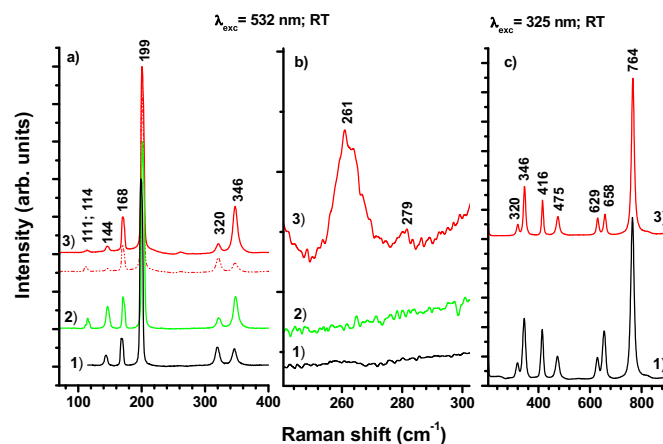


Fig. 4. (a) Raman spectra obtained with visible excitation ( $532 \text{ nm}$ ) for the undoped, lightly doped and heavily doped fibres, spectrum 1, 2 and 3, respectively. The dashed line in spectrum 3 corresponds to different sample orientation (parallel and normal to the plane of polarization). (b) Expanded region of the Raman spectra obtained with visible excitation. (c) UV ( $325 \text{ nm}$ ) Raman spectra for the same set of samples.

**Table 1**  
Raman frequencies of undoped and Eu-doped  $\beta$ -Ga<sub>2</sub>O<sub>3</sub> fibres. The additional modes detected for the Eu-doped fibres are identified by an asterisk (\*).

Present work (cm <sup>-1</sup> )	Ga <sub>2</sub> O <sub>3</sub>			Eu <sub>3</sub> Ga <sub>5</sub> O <sub>12</sub>	
	Dohy et al. [23] (cm <sup>-1</sup> )	Rao et al. [24] (cm <sup>-1</sup> )	Mode assignments [23]	Middleton et al. [25] (cm <sup>-1</sup> )	Mode assignments [25]
111	111		A <sub>g</sub>		
114(*)	114		B <sub>g</sub>	113	E <sub>g</sub>
144	147	144	B <sub>g</sub>	144	E <sub>g</sub>
				159	T <sub>2g</sub>
168	169	169	A <sub>g</sub>	170	T <sub>2g</sub>
				180	T <sub>2g</sub>
				233	T <sub>2g</sub>
				239	T <sub>2g</sub>
261(*)				262	E <sub>g</sub>
279(*)				273	T <sub>2g</sub>
				291	E <sub>g</sub>
				309	T <sub>2g</sub>
320	318	317	A <sub>g</sub>		
346	346	344	A <sub>g</sub>	346	A <sub>1g</sub>
	353		B <sub>g</sub>		
				367	T <sub>2g</sub>
				407	T <sub>2g</sub>
416	415	416	A <sub>g</sub>	415	E <sub>g</sub>
475	475	472	A <sub>g</sub> , B <sub>g</sub>		
				507	T <sub>2g</sub>
				523	A <sub>1g</sub>
				580	T <sub>2g</sub>
				595	T <sub>2g</sub>
629	628	629	A <sub>g</sub>		
	651		B <sub>g</sub>		
658	657	654	A <sub>g</sub>		
				674	E <sub>g</sub>
				736	A <sub>1g</sub>
764	763	767	A <sub>g</sub>		

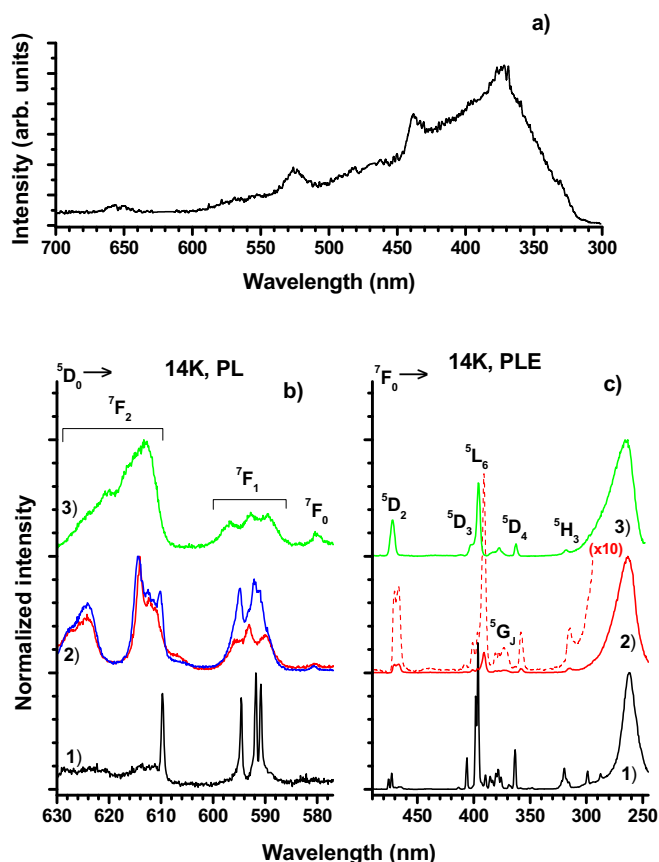
incidence. The changes in the intensity ratios of the vibrational frequencies due to local polarization effects (dashed lined spectra 3) indicate a strong anisotropy, confirming the textured nature of the fibres [23].

Fig. 5 shows the low temperature luminescence spectra of the undoped and Eu doped fibres taken at 14 K. Exciting the undoped sample with photons of 260 nm (4.77 eV), the emission is dominated by a broad ultraviolet band peaked at 377 nm overlapped by minor luminescence bands near 438 nm and 526 nm (Fig. 5a). This luminescence spectrum is very similar to that previously reported by Zhang et al. [26] in  $\beta$ -Ga<sub>2</sub>O<sub>3</sub> single crystals grown by the same LFZ technique. For Eu doped fibres (Fig. 5b) the characteristic orange/red luminescence due to the transitions between the <sup>5</sup>D<sub>0</sub> and <sup>7</sup>F<sub>1</sub> multiplets was detected. For heavily doped samples grown at 10 mm h<sup>-1</sup> (spectrum 1) containing the two crystalline phases ( $\beta$ -Ga<sub>2</sub>O<sub>3</sub> and Eu<sub>3</sub>Ga<sub>5</sub>O<sub>12</sub>), well defined sharp lines (~1 nm of full width at half maximum) are detected at 591 nm, 592 nm and 595 nm (spectrum 1) originated from the level of the <sup>5</sup>D<sub>0</sub> state and terminating on the crystal field split states of the <sup>7</sup>F<sub>1</sub> manifold. This magnetic dipole emission is the most intense one and for the hypersensitive <sup>5</sup>D<sub>0</sub> → <sup>7</sup>F<sub>2</sub> transition only one line was found peaked at ~610 nm. The heavily doped fibres grown at a faster pulling rate (30 mm h<sup>-1</sup>) exhibit a distinct behaviour of the Eu<sup>3+</sup> luminescence (spectrum 2). Here, the same lines previously detected are overlapped with the inhomogeneous broaden <sup>5</sup>D<sub>0</sub> → <sup>7</sup>F<sub>1,2</sub> transitions likely due to Eu<sup>3+</sup> ions in different environments. Additionally, the integrated intensity ratio between the <sup>5</sup>D<sub>0</sub> → <sup>7</sup>F<sub>2</sub> and <sup>5</sup>D<sub>0</sub> → <sup>7</sup>F<sub>1</sub> transitions increases, suggesting that the europium ions are placed in lower symmetry sites as also indicated by the presence of the <sup>5</sup>D<sub>0</sub> → <sup>7</sup>F<sub>0</sub> line. The former spectrum well matches the one observed for the ions inside the cubic Eu<sub>3</sub>Ga<sub>5</sub>O<sub>12</sub> as reported by Van der Ziel and Van Uitert [27]. In this case, the splitting of the J = 1 state in three components and the absence of forbidden <sup>5</sup>D<sub>0</sub> → <sup>7</sup>F<sub>0</sub> transition is

in line with the expected results for the ions in dodecahedral sites with D<sub>2</sub> local symmetry [28,29]. Moreover, rare earth (RE) ions in RE<sub>3</sub>Ga<sub>5</sub>O<sub>12</sub> hosts are known to occupy multi-sites with the RE ions in non-regular sites due to distortions of local symmetry [27–30].

The similarity of the obtained spectra for the heavily doped LFZ grown samples either at 10 mm h<sup>-1</sup> or 30 mm h<sup>-1</sup> (spectra 1 and 2) with those obtained by Daldosso et al. [29] for nanocrystalline Gd<sub>3</sub>Ga<sub>5</sub>O<sub>12</sub> also doped with europium ions, suggest that the main emitting europium ions are located in the europium gallium garnet crystalline phase. On the other hand, for the lightly doped fibres, for which no Eu<sub>3</sub>Ga<sub>5</sub>O<sub>12</sub> crystalline phase was detected either by XRD and Raman spectroscopy, noticed spectral changes of the intraionic luminescence (spectrum 3) were identified, suggesting that the main emission is originated from Eu<sup>3+</sup> ions in  $\beta$ -Ga<sub>2</sub>O<sub>3</sub> host. The presence of the <sup>5</sup>D<sub>0</sub> → <sup>7</sup>F<sub>0,1,2</sub> transitions and their intensity ratios indicate that the europium ions are placed in lower symmetry sites. The inhomogeneous broadening of the lines observed for this lightly doped fibre, is consistent with the presence of the Eu<sup>3+</sup> ions in low symmetry sites with an inhomogeneous environment, probably due to the fibre polycrystalline structure.

The identification of the different Eu<sup>3+</sup> centres was further assessed by low temperature PLE and wavelength dependent PL measurements. PLE allows identifying the excitation population mechanisms which give rise to europium luminescence in doped fibres. The normalized PLE spectra monitored at the <sup>5</sup>D<sub>0</sub> → <sup>7</sup>F<sub>2</sub> transition are shown in Fig. 5c. The spectra were normalized to the broad ultraviolet excitation band, from where all the Eu-centres are preferentially populated. Additionally, all the centres could be excited via the upper energetic levels of the Eu<sup>3+</sup> ions which exhibit slight wavelength deviations as expected for different europium environments. Spectra 2 in Fig. 5b allow to the identification that distinct Eu centres could be preferentially excited with photons with different wavelengths.



**Fig. 5.** 14 K PL spectra excited with 260 nm photons of the (a) undoped fibre grown at  $30 \text{ mm h}^{-1}$ , (b) heavily doped fibre grown at  $10 \text{ mm h}^{-1}$  (spectrum 1) and  $30 \text{ mm h}^{-1}$  (spectrum 2, red line). The blue line in spectrum 2 was obtained under resonant excitation at 390 nm, corresponding to a PLE maximum assigned to the  ${}^7F_0 \rightarrow {}^5L_6$  transition. Spectrum 3 corresponds to the lightly doped fibre grown at  $30 \text{ mm h}^{-1}$ . (c) 14 K PLE spectra of the same fibres monitored on the  ${}^5D_0 \rightarrow {}^7F_2$  transition.

#### 4. Conclusions

Undoped  $\beta\text{-Ga}_2\text{O}_3$  LFZ grown fibres and intentionally doped with 0.1 and 3 mol% of europium were produced at two different pulling rates ( $10$  and  $30 \text{ mm h}^{-1}$ ). The structural analysis using XRD and Raman measurements indicate that, regardless the pulling rate, only the  $\beta\text{-Ga}_2\text{O}_3$  crystalline phase is present in the undoped and lightly doped samples. For heavily doped samples, an additional  $\text{Eu}_3\text{Ga}_5\text{O}_{12}$  crystalline phase was identified. SEM/EDS and PIXE analysis show that europium rich regions are present in the latter fibres, corresponding to the europium gallium garnet phase. Low temperature PL measurements for the heavily doped samples evidence that most of the emitting europium ions are in the garnet structure in different local site symmetries and/or environments. Sharp  $\text{Eu}^{3+}$  lines were assigned to europium ions in dodecahedral symmetry and other two centres were visualized with the ions in lower site symmetry. On the other hand, for lightly doped samples, the intraionic lines are inhomogeneously broader with a spectral shape of the emitting ions different than those observed for the europium gallium garnet phase. The  $\text{Eu}^{3+}$  luminescence from the ions in  $\beta\text{-Ga}_2\text{O}_3$  host is characterized by the presence of the  ${}^5D_0 \rightarrow {}^7F_{0,1,2}$  transitions, suggesting that the ions are placed in lower symmetry sites.

#### Acknowledgement

The authors acknowledge FCT for the financial funding from PTDC/CTM/66195/2006 project and PTDC/CTM/100756/2008 projects.

#### References

- [1] H.H. Tippins, Optical absorption and photoconductivity in the band edge of  $\beta\text{-Ga}_2\text{O}_3$ , *Phys. Rev.* **A140** (1965) 316–319.
- [2] M. Passlack, E.F. Schubert, W.S. Hobson, M. Hong, N. Moriya, S.N.G. Chu, K. Konstadinidis, J.P. Mannaerts, M.L. Schnoes, G.J. Zyzdik,  $\text{Ga}_2\text{O}_3$  films for electronic and optoelectronic applications, *J. Appl. Phys.* **77** (1995) 686–693.
- [3] N. Ueda, H. Hosono, R. Waseda, H. Kawazoe, Anisotropy of electrical and optical properties in  $\beta\text{-Ga}_2\text{O}_3$  single crystals, *Appl. Phys. Lett.* **71** (1997) 933–935.
- [4] M. Mohamed, C. Janowitz, I. Unger, R. Manzke, Z. Galazka, R. Uecker, R. Fornari, J.R. Weber, J.B. Varley, C.G. Van de Walle, The electronic structure of  $\beta\text{-Ga}_2\text{O}_3$ , *Appl. Phys. Lett.* **97** (2010) 211903(1)–211903(3).
- [5] S. Geller, Crystal structure of  $\beta\text{-Ga}_2\text{O}_3$ , *J. Chem. Phys.* **33** (1960) 676–684.
- [6] M.R. Lorenz, J.F. Woods, R.J. Gambino, Some electrical properties of the semiconductor  $\beta\text{-Ga}_2\text{O}_3$ , *J. Phys. Chem. Sol.* **28** (1967) 403–404.
- [7] J.B. Varley, J.R. Weber, A. Janotti, C.G. Van de Walle, Oxygen vacancies and donor impurities in  $\beta\text{-Ga}_2\text{O}_3$ , *Appl. Phys. Lett.* **97** (2010) 142106(1)–142106(3).
- [8] G. Blasse, A. Bril, Some observations on the luminescence of  $\beta\text{-Ga}_2\text{O}_3$ , *J. Phys. Chem. Sol.* **31** (1970) 707–711.
- [9] T. Harwig, F. Kellendonk, S. Slappendel, The ultraviolet luminescence of  $\beta\text{-galliumsesquioxide}$ , *J. Phys. Chem. Sol.* **39** (1978) 675–680.
- [10] L. Binet, D. Gourier, Origin of the blue luminescence of  $\beta\text{-Ga}_2\text{O}_3$ , *J. Phys. Chem. Sol.* **59** (1998) 1241–1249.
- [11] T. Xiao, A.H. Kitai, G. Liu, A. Nakua, J. Barbier, Thin film electroluminescence in highly anisotropic oxide materials, *Appl. Phys. Lett.* **72** (1998) 3356–3358.
- [12] T. Miyata, T. Nakatani, T. Minami, Gallium oxide as host material for multicolor emitting phosphors, *J. Lumin.* **87–89** (2000) 1183–1185.
- [13] J. Hao, M. Cocivera, Optical and luminescent properties of undoped and rare-earth-doped  $\text{Ga}_2\text{O}_3$  thin films deposited by spray pyrolysis, *J. Phys. D: Appl. Phys.* **35** (2002) 433–438.
- [14] P. Wellenius, E.R. Smith, S.M. LeBoeuf, H.O. Everitt, J.F. Muth, Optimal composition of europium gallium oxide thin films for device applications, *J. Appl. Phys.* **107** (2010) 103111(1)–103111(5).
- [15] J. Hao, Z. Lou, I. Renaud, M. Cocivera, Electroluminescence of europium-doped gallium oxide thin films, *Thin Solid Film* **467** (2004) 182–185.
- [16] P. Gollakota, A. Dhawan, P. Wellenius, L.M. Lunardi, J.F. Mutha, Y.N. Saripalli, H.Y. Peng, H.O. Everitt, Optical characterization of Eu-doped  $\beta\text{-Ga}_2\text{O}_3$  thin films, *Appl. Phys. Lett.* **88** (2006) 221906(1)–221906(3).
- [17] P. Wellenius, A. Suresh, J.V. Foreman, H.O. Everitt, J.F. Muth, A visible transparent electroluminescent europium doped gallium oxide device, *Mater. Sci. Eng. B* **146** (2008) 252–255.
- [18] J.S. Kim, H.E. Kim, H.L. Park, G.C. Kim, Luminescence intensity and color purity enhancement in nanostructured  $\beta\text{-Ga}_2\text{O}_3\text{:Eu}^{3+}$  phosphors, *Sol. St. Commun.* **132** (2004) 459–463.
- [19] E. Nogales, J.Á. García, B. Méndez, J. Piqueras, Doped gallium oxide nanowires with waveguiding behavior, *Appl. Phys. Lett.* **91** (2007) 133108(1)–133108(3).
- [20] H. Xie, L. Chen, Y. Liu, K. Huang, Preparation and photoluminescence properties of Eu-doped  $\alpha\text{-}$  and  $\beta\text{-Ga}_2\text{O}_3$  phosphors, *Sol. St. Commun.* **141** (2007) 12–16.
- [21] E. Nogales, B. Méndez, J. Piqueras, J.A. Garcia, Europium doped gallium oxide nanostructures for room temperature luminescent photonic devices, *Nanotechnology* **20** (2009) 115201(1)–115201(5).
- [22] H. Zhu, R. Li, W. Luoab, X. Chen,  $\text{Eu}^{3+}$ -doped  $\beta\text{-Ga}_2\text{O}_3$  nanophosphors: annealing effect, electronic structure and optical spectroscopy, *Phys. Chem. Chem. Phys.* **13** (2011) 4411–4419.
- [23] D. Dohy, G. Lucazeau, Raman spectra and valence force field of single-crystalline  $\beta\text{-Ga}_2\text{O}_3$ , *J. Sol. St. Chem.* **45** (1982) 180–192.
- [24] R. Rao, A.M. Rao, B. Xu, J. Dong, S. Sharma, M.K. Sunkara, Blueshifted Raman scattering and its correlation with the [110] growth direction in gallium oxide nanowires, *J. Appl. Phys.* **98** (2005) 094312(1)–094312(5).
- [25] R.C. Middleton, D.V.S. Muthu, M.B. Kruger, High-pressure spectroscopic studies of europium gallium and gadolinium aluminum garnets, *Sol. St. Commun.* **148** (2008) 310–313.
- [26] J. Zhang, B. Li, C. Xia, G. Pei, Q. Deng, Z. Yang, W. Xu, H. Shi, F. Wu, Y. Wu, J. Xu, Growth and spectral characterization of  $\beta\text{-Ga}_2\text{O}_3$  single crystals, *J. Phys. Chem. Sol.* **67** (2006) 2448–2451.
- [27] J.P. Van der Ziel, L.G. Van Uitert, Optical emission spectrum of  $\text{Cr}^{3+}\text{-Eu}^{3+}$  pairs in europium gallium garnet, *Phys. Rev.* **186** (1969) 332–339.
- [28] L.C. Courrol, L. Gomes, A. Brenier, C. Pédriani, C. Madej, G. Boulon, Optical detection of  $\text{Eu}^{3+}$  sites in  $\text{Gd}_3\text{Ga}_5\text{O}_{12}\text{:Eu}^{3+}$ , *Rad. Eff. Def. Sol.: Inc. Plas. Sci. Plas. Tech.* **135** (1995) 81–84.
- [29] M. Daldosso, D. Falcomer, A. Speghini, P. Ghigna, M. Bettinelli, Synthesis, EXAFS investigation and optical spectroscopy of nanocrystalline  $\text{Gd}_3\text{Ga}_5\text{O}_{12}$  doped with  $\text{Ln}^{3+}$  ions ( $\text{Ln} = \text{Eu}, \text{Pr}$ ), *Opt. Mater.* **30** (2008) 1162–1167.
- [30] V. Lupei,  $\text{RE}^{3+}$  emission in garnets: multisites, energy transfer and quantum efficiency, *Opt. Mater.* **19** (2002) 95–107.